

Catalytic Biochar and Refuse-Derived Char for the Steam Reforming of Waste Plastics Pyrolysis Volatiles for Hydrogen-Rich Syngas

Yukun Li and Paul T. Williams*



Cite This: *Ind. Eng. Chem. Res.* 2023, 62, 14335–14348



Read Online

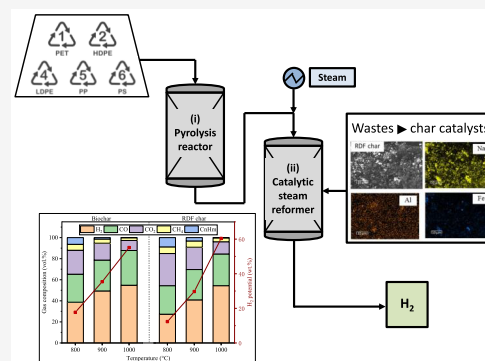
ACCESS |

Metrics & More

Article Recommendations

ABSTRACT: High-density polyethylene (HDPE) was pyrolyzed in a fixed-bed reactor and the derived pyrolysis volatiles passed directly to a second-stage fixed-bed reactor for catalytic steam reforming with the aim to produce hydrogen-rich syngas. The catalysts used were biochar produced from the pyrolysis of waste biomass and solid waste char produced from the pyrolysis of processed municipal solid waste in the form of refuse-derived fuel (RDF). The influence of char catalyst temperature and steam input were used to optimize the production of H₂ syngas. Other types of waste plastics (low-density polyethylene (LDPE), polypropylene (PP), polystyrene (PS), and poly(ethylene terephthalate) (PET)) were also investigated to compare with the production from HDPE. The highest yields of syngas (H₂, CO) were produced at 3.83 g g_{plastic}⁻¹ for biochar as the catalyst and 2.73 g g_{plastic}⁻¹ for RDF char as the catalyst, when the steam input was 10 g h⁻¹ g_{catalyst}⁻¹ and catalyst temperature was 1000 °C.

Increasing amounts of steam input also increased the syngas yield, but at high steam inputs, saturation of the catalyst reduced syngas yield. Of the different plastic types investigated, the polyolefin plastics (HDPE, LDPE, PP) produced the highest yield of syngas, whereas PS and PET yields were significantly lower in the presence of both biochar and RDF char catalysts. Hydrogen yields were ~0.44 g g_{plastic}⁻¹ for the polyalkene plastics with the biochar catalyst but were only ~0.32 g g_{plastic}⁻¹ with the RDF char catalyst. At 1000 °C, the H₂ potential from the processing of plastic with RDF char as the catalyst was higher than with biochar as the catalyst, which was attributed to the higher presence of an inorganic metal in the RDF char possessing catalytic properties.

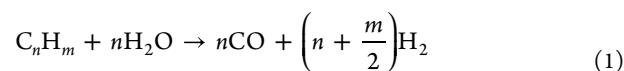


1. INTRODUCTION

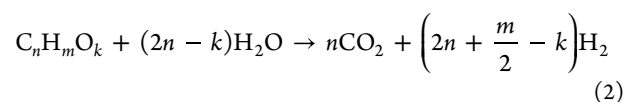
Current worldwide production of plastics is approaching 400 million tonnes per year and after the service lifetime of plastic products in their various end-use applications, they will become waste plastics.^{1,2} Most waste plastics are largely recycled via mechanical methods but there is increasing interest to produce higher-value products from plastic waste. For example, thermochemical routes to produce liquid fuels, chemicals, new carbon nanomaterials, and hydrogen have been investigated.^{3–6} Of particular interest is the production of hydrogen from waste plastics in that it is regarded as a future zero-carbon fuel with potential to mitigate the impacts of global warming and the consequent damage of environmental climate change. The focus of the work presented here is the production of hydrogen from waste plastics using a two-stage thermochemical process of pyrolysis-catalytic steam reforming. Such two-stage pyrolysis reforming reactor systems have been recently reported.^{4–9} The process first involves pyrolysis of the waste plastics followed by catalytic steam reforming of the evolved pyrolysis volatiles. The pyrolysis of polyolefin plastics (high-density polyethylene (HDPE), low-density polyethylene (LDPE), and polypropylene (PP)) generates a suite of hydrocarbons (C_nH_m). However, pyrolysis of polystyrene (PS) produces mainly aromatic volatiles, and poly(ethylene

terephthalate) (PET) will also produce oxygenated hydrocarbons (C_nH_mO_k). The range of evolved pyrolysis volatiles then undergo catalytic steam reforming reactions in the second-stage reactor (eqs 1 and 2)

Hydrocarbons steam reforming:



Oxygenated hydrocarbons steam reforming:



The evolved CO will also undergo reaction with the input steam to produce further hydrogen via the water–gas shift reaction

Received: July 6, 2023

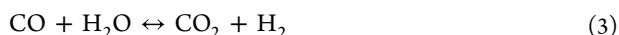
Revised: August 17, 2023

Accepted: August 17, 2023

Published: August 29, 2023



Water-gas shift:



Conventional catalysts used in the catalytic steam reforming process are typically prepared using a porous catalyst support loaded with suitable catalytic metals (such as Ni, Fe, Cu, Ca, etc.) to enhance reforming reactions for improved hydrogen production during the reforming stage.^{10–13} However, these catalysts may suffer from deactivation due to carbonaceous deposits, which block the pore structure and hinder the interaction between the active phase and reactants. To address this problem, the use of pyrolysis char as a catalyst for the catalytic steam reforming process has been the topic of recent studies; for example, biochar, coal char, and tire char have been proposed as potential catalysts.^{14–16} The advantages of pyrolysis chars as catalysts have been reported as their high surface area and pore volume, and the presence of abundant surface functional groups also regarded as low-cost catalysts.^{14,15,17} In addition, the metals present, as the ash component of the char, can act as catalysts to enhance hydrogen and syngas yield via the reforming and water–gas shift reactions.¹⁴ For example, alkaline metals such as K, Na, and Ca found in biochars and transition metals such as Fe, Co, Cu, and Zn found in coal and tire chars have been reported as active metals for the promotion of steam reforming and water–gas shift reactions.^{14–19} Yao et al.¹³ investigated the use of biochar produced from the pyrolysis of different biomass types as a support for nickel and reported that the texture and compositional characteristics of the biochar catalysts promoted the reforming of pyrolysis volatiles derived from biomass. Liu et al.²⁰ used biochar from the pyrolysis and steam activation of biomass and also showed that the presence of O-containing functional groups in the biochar promoted the steam reforming process. Klinghoffer et al.²¹ examined the effect of the presence of inorganic compounds (Ca, K, Na, P, Si, Mg) on hydrocarbon cracking reactions. They showed that removal of the elements by acid washing significantly reduced the catalytic activity of the biochar. Wang et al.²² used a two-stage pyrolysis reforming process with a Ni-based biochar catalyst for the production of hydrogen-rich syngas. The biochar performed effectively as a steam reforming catalyst, but the presence of Ni increased the yield of hydrogen and syngas.

In addition to biochar, other carbonaceous materials have been used to produce chars via pyrolysis for subsequent use as steam reforming catalysts. Coal-derived pyrolysis char has been used as a Ni support material for the two-stage pyrolysis reforming of biomass to produce high-yield hydrogen syngas.²³ Waste tires have been used to produce a char catalyst for the catalytic steam reforming of biomass pyrolysis volatiles, and hydrogen yields of $0.08 \text{ g g}_{\text{biomass}}^{-1}$ were reported.²⁴

A further advantage of using pyrolysis chars as catalysts is the potential to use process conditions that allow the char to act as a reactant as well as a catalyst.^{18,19} Thereby, the carbonaceous char is also gasified in the presence of steam to generate hydrogen and carbon monoxide and consequently increases the overall yield of hydrogen and syngas (eqs 4–6)

Water-gas (primary):



Water-gas (secondary):



Boudouard:



In summary, pyrolysis char (including biochar, coal char, and tire char) has been extensively studied in the process of catalytic steam reforming of biomass pyrolysis volatiles and has shown excellent catalytic properties. However, there is still limited investigation into the application of pyrolysis char in the catalytic steam reforming of waste plastics. Our previous study¹⁸ highlighted the high catalytic activity of pyrolysis tire char in the catalytic steam reforming of plastics. For example, high yields of hydrogen were reported from the processing of the HDPE at $0.27 \text{ g H}_2 \text{ g}_{\text{plastic}}^{-1}$ and syngas (H_2 , CO) yields of $2.85 \text{ g g}_{\text{plastic}}^{-1}$ at a char catalyst/HDPE ratio of 1:1. At higher char catalyst/HDPE ratio (4:1), a H_2 yield of $0.42 \text{ g g}_{\text{plastic}}^{-1}$ and syngas yield of $4.59 \text{ g g}_{\text{plastic}}^{-1}$ were reported. Nevertheless, there is a lack of research on the catalytic steam reforming of waste plastics using biochar and refuse-derived fuel (RDF) char. To address this gap, this work focuses on the two-stage pyrolysis-catalytic steam reforming of waste plastics to investigate the effects of biochar and RDF char on the catalytic process and catalytic products. The two char catalysts were produced from the pyrolysis of waste biomass and processed municipal solid waste (MSW) in the form of refuse-derived fuel (RDF) where the noncombustible components of the MSW, such as glass and metal components, have been removed. The influence of different process conditions and the use of different types of plastic as the feedstock are reported. This work represents for the first time that a municipal solid waste pyrolysis char has been investigated as a catalyst for catalytic steam reforming of volatiles produced from waste plastics. In particular, in addition to assessing the influence of char type acting as a steam reforming catalyst, the process conditions are formulated to gasify the char catalyst to produce enhanced hydrogen and syngas yield; thereby, the char catalyst is deliberately consumed during the process.

2. MATERIALS AND METHODS

2.1. Materials. The plastics used in the experiments were HDPE, LDPE, PP, PS, and PET. HDPE, PP, and PS were obtained from Regain Polymers Limited, Castleford, U.K., while LDPE and PET were purchased from Sigma-Aldrich. All of the plastics were subjected to ultimate analysis and proximate analysis, and the results have been reported in our previous work.¹⁹

The biomass used as feedstock for the production of the biochar catalyst was waste wood sawdust with a particle size of 1 mm and was obtained from Liverpool Wood Pellets Ltd., Liverpool, U.K. The waste-derived municipal solid waste feedstock was in the form of refuse-derived fuel (RDF) pellets. Waste-derived fuels include RDF and also solid recovered fuel (SRF) produced from MSW typically in mechanical-biological treatment plants. SRF complies with the standards established within the European Union by the European Committee for Standardization (CEN), while RDF does not follow such stringent quality management procedures; therefore, its component content and quality may be more variable.²⁵ The RDF was obtained from a UK municipal waste treatment plant in NE England. The char catalysts were produced from the pyrolysis of biomass and RDF at a final temperature of $800 \text{ }^\circ\text{C}$ in a fixed-bed stainless steel reactor described in our previous work.¹⁸ The pyrolysis process was as follows: biomass and RDF were heated from room temperature to $800 \text{ }^\circ\text{C}$ at $20 \text{ }^\circ\text{C}$

min^{-1} in the pyrolysis reactor and maintained at that temperature for 20 min. The pyrolysis of the biomass and RDF was undertaken several times to generate enough char for the experiments that produced mean biochar yields of 23.9 wt % and mean RDF char yields of 19.9 wt %.

2.2. Experimental Reactor System. A schematic diagram of the pyrolysis-catalytic steam reforming reactor system used in the experiments is shown in Figure 1. The system included a

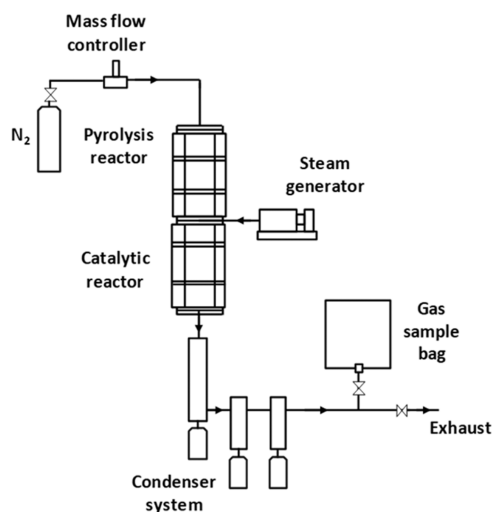


Figure 1. Schematic diagram of the two-stage pyrolysis-catalytic steam reforming reaction system.

first-stage pyrolysis reactor, a second-stage catalytic steam reforming reactor, a steam supply system, condenser system, and gas collection system. The two reactors were constructed of stainless steel and were independently heated by external electrical furnaces: the first reactor had dimensions of 200 mm \times 40 mm diameter and the second had 300 mm \times 22 mm diameter. The experimental procedure was as follows: 1 g of plastic and 1 g of catalyst were placed in the middle of the pyrolysis reactor and catalytic reactor, respectively. N_2 was injected continuously (100 mL min^{-1}) to discharge the air in the reactor and as a carrier gas to sweep the evolved product gases through the reactor system. Digital flowmeters were used to measure the inlet and exit gas flows. The catalytic reactor was first heated to the desired temperature, and then the pyrolysis reactor was heated from room temperature to $600 \text{ }^\circ\text{C}$ at a heating rate of $20 \text{ }^\circ\text{C min}^{-1}$. It is worth noting that in the pyrolysis-catalytic steam reforming process, the volatile stream generated from pyrolysis is not condensed but directly enter the catalytic reforming stage. After the steam reforming reaction, the gas entered the three-stage cooling system, where the condensable gas was cooled and collected in the condenser, and the noncondensable gases entered a Tedlar gas sample bag.

2.3. Product Analysis and Characterization. Gas products collected from the pyrolysis-catalytic steam reforming of the waste plastics were analyzed immediately after each experiment using three independent packed column Varian CP-3380 gas chromatographs. The first analyzed C_1 – C_4 hydrocarbons on a 60–80 mesh column, N_2 carrier gas, and FID; the second analyzed H_2 , CO , O_2 , and N_2 on a HayeSep 80–100 mesh column, Ar carrier gas, and TCD; the third analyzed CO_2 on a HayeSep 80–100 mesh column, Ar carrier gas, and TCD.

Raw feedstock materials, fresh catalysts, and used catalysts were characterized by several instruments. The ultimate analysis of the samples was carried out using an elemental analyzer (Flash EA2000). The proximate analysis was conducted using a Mettler Toledo proximate analyzer. Sequential acid digestion was done using HNO_3 followed by $\text{HCl}/\text{H}_2\text{SO}_4$ and atomic absorption spectrometry (AAS) using a Varian fast sequential atomic absorption spectrophotometer (Varian AA240FS). The fresh catalysts were characterized by X-ray diffraction (XRD) on a Bruker D8 instrument to identify the crystallographic structures and composition. The analysis range (2θ) was 10 – 80° with a scanning step of 0.05° . A Hitachi SU8230 scanning electron microscope (SEM) coupled with energy dispersive X-ray spectrometry (EDXS) was used to characterize the surface morphology and element distribution of the catalysts.

2.4. Reaction Indices. The total gas yield, gas concentration, yield of each gas, and the ratio of experimental H_2 yield to theoretical H_2 yield (H_2 potential) were used to evaluate the efficiency of the pyrolysis-catalytic steam reforming process. The calculation formulae were as follows

$$\text{gas yield}_{\text{total}} (\text{wt } \%) = \frac{\sum m_{\text{each gas}}}{m_{\text{plastic}} + m_{\text{water}} + m_{\text{reacted char}}} \quad (7)$$

$$\text{gas yield}_{\text{each gas}} (\text{g g}^{-1}_{\text{plastic}}) = \frac{V_{\text{each gas}}}{22.4} \times M_{\text{each gas}} / m_{\text{plastic}} \quad (8)$$

$$\text{H}_2 \text{ potential } (\%) = \frac{\text{experimental H}_2 \text{ yield}}{\text{theoretical H}_2 \text{ yield}} \quad (9)$$

where $m_{\text{each gas}}$ represents the mass of each gas, $M_{\text{each gas}}$ represents the molar mass of each gas, m_{plastic} represents the mass of plastic, m_{water} represents the mass of water, $m_{\text{reacted char}}$ represents the mass of reacted char, and $V_{\text{each gas}}$ represents the volume of each gas. The maximum theoretical hydrogen yield includes hydrogen from plastics and char, calculated based on the concept proposed by Czernik and French.²⁶ The calculation assumes that all of the carbon and hydrogen in the raw feedstock materials were converted into carbon dioxide and hydrogen during the steam reforming process, including steam reforming (eqs 1 and 2) and water–gas shift (eq 3) reactions. However, in this work, the productions of hydrogen and carbon monoxide from steam–char gasification reactions (eqs 4–6) are also included.

3. RESULTS AND DISCUSSION

3.1. Characterization of Catalysts. The char catalysts used in the second-stage steam reforming were biochar and RDF char obtained from the pyrolysis of biomass and RDF. The proximate analysis, ultimate analysis, and metal analysis of the biomass, RDF, and their derived pyrolysis chars are presented in Table 1. As can be seen from Table 1, the feedstock biomass and RDF had high and similar volatile content. After pyrolysis, the volatile content of the derived pyrolysis char was only about 2% because a large amount of volatile content was converted into pyrolysis oil during the char catalyst preparation stage. The yield of pyrolysis oil from the biomass and RDF was 61 and 55 wt %, respectively, which was linked to the volatile content of the biomass and RDF feedstock.²⁷

Table 1. Proximate Analysis, Ultimate Analysis, and Metal Analysis of Biomass, RDF, and Their Pyrolysis Chars^a

| properties | | biomass | biochar | RDF | RDF char |
|--|-----------|---------|---------|-------|----------|
| proximate analysis (wt %) | volatiles | 74.06 | 1.84 | 70.26 | 2.66 |
| | fixed C | 14.77 | 90.78 | 9.26 | 47.30 |
| | ash | 5.32 | 6.36 | 16.93 | 49.78 |
| ultimate analysis (wt %, dry ash-free) | C | 47.34 | 91.91 | 43.56 | 46.73 |
| | H | 4.88 | 0.53 | 1.85 | 0.60 |
| | O | 47.65 | 6.30 | 47.67 | 51.55 |
| | N | 0.14 | 1.26 | 6.93 | 0.7 |
| | S | nd | nd | nd | 0.43 |
| metal analysis (wt %) | Na | nd | nd | 0.79 | 1.24 |
| | Mg | 0.06 | 0.26 | 0.46 | 0.63 |
| | Al | nd | 0.20 | 0.91 | 2.27 |
| | K | 0.29 | 0.99 | 0.79 | 0.76 |
| | Ca | 2.67 | 4.15 | 8.44 | 10.53 |
| | Fe | 0.21 | 0.07 | 1.26 | 1.73 |

^and: not detected.

From the perspective of elemental analysis, the carbon and oxygen contents of biomass and RDF were similar, but after pyrolysis, the carbon content of biomass significantly increased, and the oxygen content significantly decreased. The carbon and oxygen content of RDF increased slightly after pyrolysis, mainly because most of the oxygen in biomass enters the pyrolysis oil, while the oxygen in RDF remains in the ash in the form of metal oxides. Mei et al.²⁸ compared the pyrolysis of municipal solid waste and biomass wheat straw and reported a similar phenomenon. The pyrolysis process also increased the metal concentration of the char. Clearly, the concentration of most metals in the RDF char was higher than that contained in the biochar. The metals in RDF char are mainly Ca, Al, and Fe, while the metals in biochar are mainly Ca and K.

Figure 2 shows the SEM-EDXS element scanning characterization of the pyrolysis-derived biochar and RDF char, which

was performed to understand the surface morphology and element distribution of the char catalysts. Figure 2a–c shows the SEM image and surface metal distribution of the biochar. It can be seen that the surface of biochar was rough, with large pore structures and cracks. K and Ca were dispersed on the surface of biochar, and the content of Ca was high, which was consistent with the previous metal analysis shown in Table 1. An overview of the composition and application of biomass ash presented by Vassilev et al.²⁹ also showed that the alkali and alkaline-earth metals (AAEM) were mainly Ca and K. The inherent AAEM species in biochar have been proven to significantly impact catalytic activities.³⁰ Figure 2d–i shows the surface morphology of the RDF char and the distribution of metal elements from SEM-EDXS analysis. The surface of the RDF char was uneven, with many small particles agglomerating together and adhering to the surface. These particles were inorganic elements in the ash that emerged after the release of volatiles from the RDF during the pyrolysis process. The metal distribution in Figure 2e–i also confirmed this view. The elements, Na, Al, K, and Ca were uniformly distributed on the carbon surface, while Fe was localized.

Figure 3 shows the XRD patterns and phase compositions of the biochar and RDF char. The XRD spectra of biochar shows that there are two wide diffraction peaks, mainly attributed to the presence of amorphous carbon in woody char. The amorphous nature of this carbon is more distinct at higher temperatures or extended residence times, eventually approximating to that of amorphous carbon.³¹ Although Figure 2 shows that K and Ca metals are distributed on the surface of the biochar, due to their low content and uniform dispersion, the corresponding peaks are weak or not obvious in the XRD spectra. Conversely, there are many sharp diffraction peaks in the XRD spectra of the RDF char. It can be observed from Figure 3 that K, Ca, Na, and Al mainly exist in RDF char in the form of $K_3Na(SO_4)_2$, $Na(AlSi_3O_8)$, and $CaCO_3$. Carbonates such as $CaCO_3$ have been reported to have a tendency to bond with carbon to form CaO. Also, it has been shown that CaO

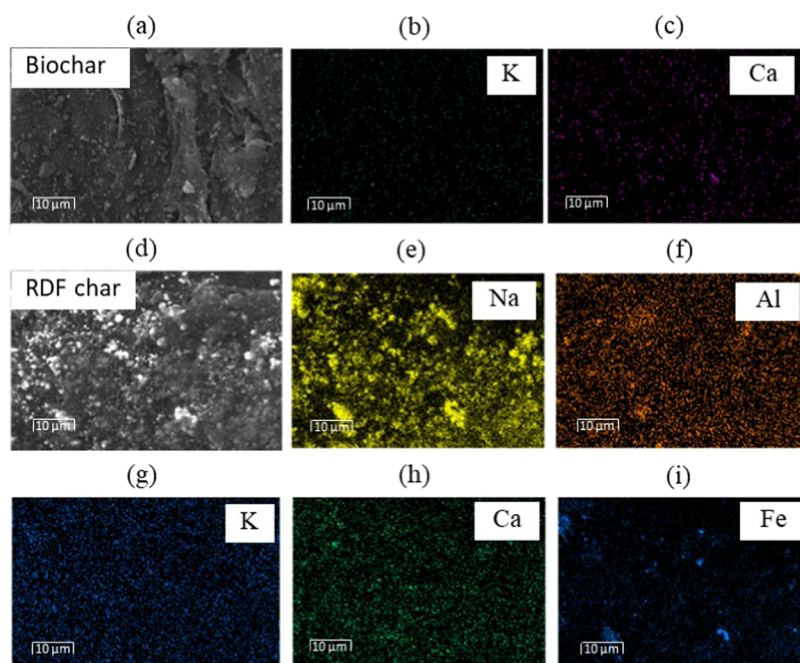


Figure 2. SEM images and elemental mapping of (a–c) biochar and (d–i) RDF char.

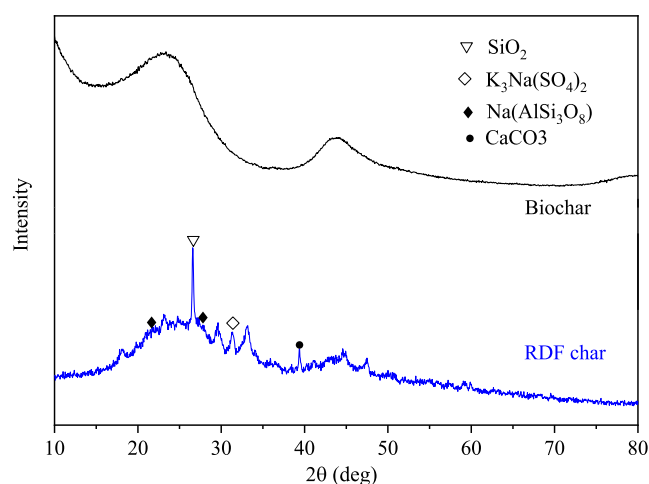


Figure 3. XRD patterns of biochar and RDF char.

shows a strong catalytic effect in relation to the cracking of aromatic rings in the pyrolysis volatiles.^{31,32} The phase composition of the RDF char is related to the original waste type and preparation conditions. Given the complex components in RDF char, its XRD pattern presents a relatively complex spectra, containing multiple diffraction peaks. For example, it has been reported that MSW char prepared at 500 °C was mainly rich in SiO₂, Na(AlSi₃O₈), CaCO₃, (Mg_{0.03}Ca_{0.97})CO₃, and other minerals.²⁸

3.2. Influence of Char Catalyst Temperature on H₂ and Syngas Yield. Temperature plays an important role in the second-stage reforming process of the volatiles derived from the pyrolysis of the plastics and also the catalytic activity of the char.³³ The chars derived from the pyrolysis of biomass and RDF were used as catalysts in the steam reforming of the hydrocarbons from the pyrolysis of HDPE to investigate their catalytic performance in relation to different catalyst temperatures of, 800, 900, and 1000 °C. The steam input to the reforming reactor as hourly weight space velocity was kept constant at 8 g h⁻¹ g_{catalyst}⁻¹. Under different catalytic conditions, the pyrolysis of waste plastics stage was maintained under the same conditions (600 °C), which made the volatiles entering the second stage the same. HDPE was almost completely converted into pyrolysis volatiles, with only a small fraction remaining as the char residue (<0.03 g). The results in terms of product yields at different catalyst temperatures with biochar and RDF char catalysts are shown in Table 2. Also shown in Table 2 is the mass of reacted char that was obtained from the mass of char catalyst used (1.0 g) minus the mass of residual reacted char in the catalyst reactor after pyrolysis-catalytic steam reforming of HDPE.

As the temperature of the char catalyst was raised from 800 to 1000 °C, the gas yield from HDPE increased from 38.1 to 56.5 wt % for biochar and from 32.7 to 46.6 wt % for the RDF char, in terms of the input mass of plastic + water + reacted char. Table 2 also shows the gas yield results for the processing of the HDPE but in terms of the mass of input plastic only, where the yields of gas are considerably higher, increasing from 3.46 g g_{plastic}⁻¹ at 800 °C catalyst temperature to 5.41 g g_{plastic}⁻¹ at 1000 °C for the biochar catalyst and from 2.92 to 4.35 g g_{plastic}⁻¹ for the RDF char catalyst. Reporting the gas yields in relation to the mass of plastic only may be considered a legitimate and interesting presentation of the results, since the input water for the generation of the steam would be low-cost and the char catalyst that is consumed in the process would also be regarded as a low-cost material. Similarly, Table 2 shows the yield of syngas in terms of the mass of input plastic only, where very high yields of syngas were found at a high temperature of 1000 °C, of 3.73 g g_{plastic}⁻¹ for the biochar catalyst, and 2.71 g g_{plastic}⁻¹ for the RDF char catalyst.

The results clearly show that for both the biochar and RDF char catalysts, increased temperature promoted the conversion of the hydrocarbons of the HDPE pyrolysis volatiles into gases. Thereby, the endothermic steam reforming reaction and char-steam gasification reaction were promoted at higher temperatures.³⁴ The carbon of the char catalyst was consumed during the process via steam-char gasification reactions that increased at higher temperatures. This was confirmed by the increase of the mass of char that was reacted in the process in relation to the increase of the char catalyst temperature (Table 2). It is worth noting that when the catalyst temperature was 1000 °C, all of the biochar carbon was consumed in the steam-char gasification process.

The gas yield results were also determined as the total mass of gas generated in grams. As the catalyst temperature was increased from 800 to 900 °C, the total mass of gas increased by 1 g, and the mass of the biochar participating in the reaction increased by 0.53 g, i.e., from 0.28 to 0.81 g. At 1000 °C, the total mass of gas generated increased by a further ~1 g; however, the mass of biochar involved in the reaction increased by 0.19 g, i.e., 1.0 g of char catalyst was consumed. This indicated that the increase in gas yield from 900 to 1000 °C was mainly caused by the steam reforming of hydrocarbons, i.e., the hydrocarbons reacted more fully at high temperatures. This phenomenon was also demonstrated by the relationship between the mass of the RDF char involved in the reaction and the mass of the generated gas as the catalyst temperature was increased. The steam reforming of the pyrolysis volatile components of plastic takes place mainly at catalyst temperatures between 700 and 900 °C in the presence of different catalysts. This temperature range is reported to be effective for

Table 2. Product Yields and Amount of Char Reacted from Pyrolysis-Catalytic Steam Reforming of HDPE at Different Temperatures with the Presence of Biochar and RDF Char

| temperature (°C) | 800 | | 900 | | 1000 | |
|---|---------|----------|---------|----------|---------|----------|
| | biochar | RDF char | biochar | RDF char | biochar | RDF char |
| catalyst | | | | | | |
| gas yield in relation to plastic + water + reacted char (wt %) | 38.1 | 32.7 | 45.7 | 41.2 | 56.5 | 46.6 |
| liquid yield in relation to plastic + water + reacted char (wt %) | 68.0 | 78.7 | 50.8 | 66.3 | 38.9 | 48.9 |
| mass balance (wt %) | 106.2 | 111.9 | 97.0 | 108.1 | 95.7 | 96.0 |
| gas yield (g g _{plastic} ⁻¹) | 3.46 | 2.92 | 4.45 | 3.7 | 5.41 | 4.35 |
| syngas yield (g g _{plastic} ⁻¹) | 1.35 | 0.94 | 2.36 | 1.66 | 3.73 | 2.71 |
| char reacted (g) | 0.28 | 0.25 | 0.81 | 0.45 | 1 | 0.62 |

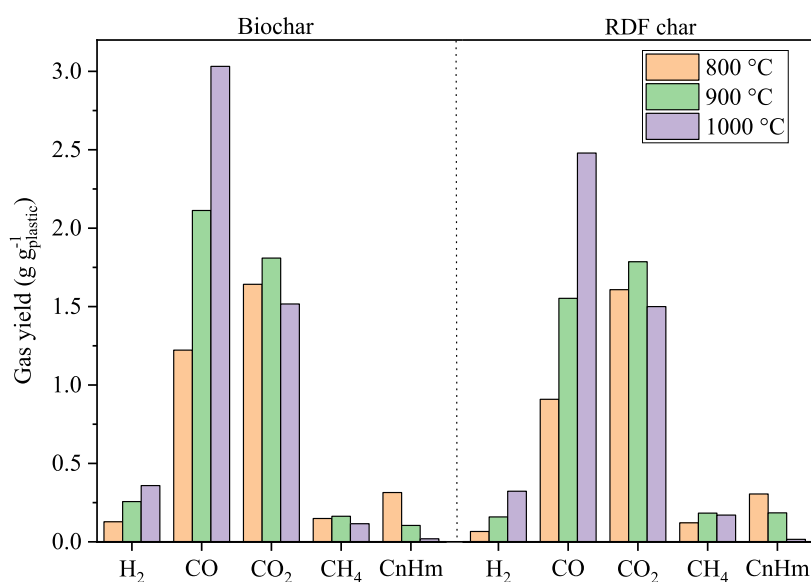


Figure 4. Individual gas yield from pyrolysis-catalytic steam reforming of HDPE at different temperatures in the presence of biochar and RDF char catalysts.

the steam reforming of light organic components but not high enough for steam reforming of heavy organic compounds.⁸ Wu et al.³⁵ investigated the conversion under partial oxidation conditions of biomass-derived tar in a two-stage continuous reactor at temperatures of 700–1100 °C. They reported that the yield of pyrolysis tar was almost linearly decreased from 19.98 to 2.1 wt % when the temperature was increased from 700 to 1100 °C, with conversion efficiencies of 23 and 92%, respectively. Removal of heavy tars by steam reforming at high temperatures (1000–1400 °C) was studied by Li et al.³⁶ who proposed that increasing the temperature could accelerate the cracking of heavy tar, as was also the case with the introduction of moderate amounts of steam.

Figure 4 shows the individual gas yields produced from the pyrolysis-catalytic steam reforming of HDPE at different char catalyst temperatures with biochar and RDF char. The H₂ yield from the processing of HDPE with the biochar catalyst increased linearly from 0.13 to 0.36 g g_{plastic}⁻¹ as the catalyst temperature was increased from 800 to 1000 °C. When the temperature was raised from 800 to 900 °C, the main source of hydrogen in the case of biochar was the char–steam reaction (eqs 4–6) since most of the carbon (0.81 g) was consumed over this temperature range (Table 2). Further increase in catalyst temperature to 1000 °C showed that the steam reforming of the pyrolysis volatiles contributed most of the H₂ yield, the high temperature enhancing the steam reforming of the heavy hydrocarbons.³⁷ The yield of CO also increased with the increase in temperature, and its source is mainly the steam reforming of hydrocarbons and the reaction of char and steam. The CO₂ yield increased moderately from 1.64 to 1.81 g g_{plastic}⁻¹ when the catalyst temperature was increased from 800 to 900 °C, perhaps due to the water–gas shift reaction. However, with a further temperature increase to 1000 °C, the yield of CO₂ dropped to 1.52 g g_{plastic}⁻¹, and the yield of CO increased substantially, which was more likely attributed to the Boudouard reaction (eq 6). This phenomenon was consistent with the research of Wu et al.³⁵ who showed that under partial oxidation conditions, the CO₂ yield from biomass tar cracking was significantly increased from 8.5 to 13.6 wt % when the temperature was increased from 700 to 900 °C. With the

temperature increasing after 900 °C, the CO₂ yield decreased but other noncondensable gases continued to increase. The highest CH₄ yield was reached at 0.16 g g_{plastic}⁻¹ at 900 °C. The yield of C_nH_m showed a continuous decreasing trend with increasing temperature. This is apparently due to the increase in temperature that promoted the tar steam reforming reaction, causing it to produce CO and H₂.

The catalytic effect of the RDF char in relation to the catalyst temperature is presented in Figure 4. The individual gas yields (H₂, CO, CO₂) from pyrolysis-catalytic steam reforming of HDPE using the RDF char catalyst were lower than those using the biochar catalyst, but their trends with increasing temperature were similar. The main reason for the low gas yield was the low carbon content of RDF char that restricted the gas formation reactions via char–steam reactions (eqs 4–6). The RDF char also contained a large amount of ash (49.78 wt %), which will not react with steam. As can be seen from Table 2 and the mass of the char reacted, the biochar was fully converted to gas at 1000 °C, while 38 wt % (0.38 g) RDF char remained. Biochar and RDF char showed obvious differences in the yields of various gas products. For example, at 900 °C, biochar and RDF char acted as catalysts in the steam reforming of pyrolysis volatiles of HDPE, the yields of hydrogen being 0.13 and 0.06 g g_{plastic}⁻¹, respectively. Under the same conditions, the reported hydrogen yield from the processing of waste plastic using conventional catalysts (Ni, Fe) was 0.04–0.14 g g_{plastic}⁻¹,^{10,14,38} which fully reflected the effectiveness of biochar and RDF char as catalysts.

Volumetric gas concentration plays a vital role in engineering, allowing assessment of gas composition for tailored gas selection based on different end-use application needs. For example, a syngas mixture of high hydrogen concentration and low CO concentration can be used to produce hydrogen used for ammonia synthesis or fuel cells.³⁹ Thereby, the process of waste plastic pyrolysis coupled with catalytic steam reforming with waste-derived pyrolysis chars may be manipulated to regulate the volumetric gas composition of the product gas for determination of end-use applications. The volumetric relative gas composition with the use of biochar and RDF char catalysts for the catalytic steam reforming of HDPE pyrolysis

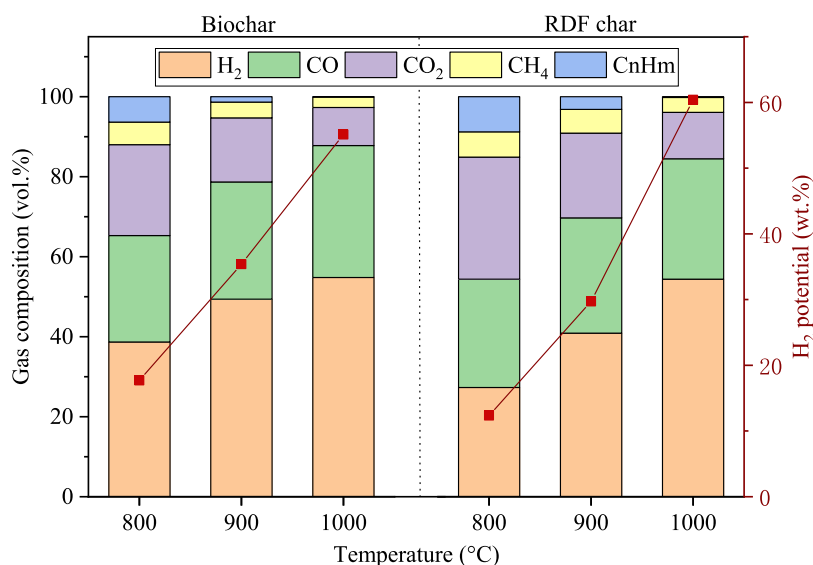


Figure 5. Volumetric gas composition and theoretical hydrogen yield production from pyrolysis-catalytic steam reforming of HDPE at different temperatures in the presence of biochar and RDF char catalysts.

volatiles at different catalyst temperatures is shown in Figure 5. The gases produced by pyrolysis were mainly composed of H₂, CO, CO₂, CH₄, and C_nH_m. When biochar was used as the catalyst, the concentration of volumetric hydrogen composition increased from 38.7 to 54.8 vol % with the increase in temperature, and the concentration of CO also showed a slight increase. The concentration of CH₄ also showed a downward trend, mainly due to the increase in H₂ and CO production, which increased the total gas volume. The concentration of C_nH_m was significantly reduced from 6.37 vol % at 800 °C to less than 0.1 vol % at 1000 °C. The quality of syngas can be improved by increasing the temperature. The volumetric concentration of syngas (H₂ + CO) produced with biochar was increased from 65 vol % at 800 °C to 88 vol % at 1000 °C. When RDF char was used as the catalyst, the concentration of each individual gas changed with temperature, similar to that when biochar was used as the catalyst, but the concentrations of H₂ and syngas in the overall gas composition was lower under the same experimental conditions. For example, when biochar was used as the catalyst, H₂ concentration and syngas concentration were 38.7 and 65.3 vol %, respectively, at 800 °C. However, when RDF char was used as the catalyst, H₂ concentration and syngas concentration were reduced to 27.3 and 54.4 vol %, respectively.

The hydrogen potential²⁶ was calculated based on the experimental yield of H₂ and on the calculated theoretical H₂ yield where the carbon and hydrogen in the feedstock plastic is all converted to H₂ via the steam reforming (eqs 1 and 2) and water–gas shift (eq 3) reactions. However, in this work, the consumption of the char catalyst during the reaction via steam–char gasification reactions (eqs 4–6) was also calculated. According to the calculation, based on the elemental analysis of the HDPE plastic and the char catalysts (Table 1), the maximum hydrogen yield from the pyrolytic volatiles of HDPE derived from the pyrolysis-catalytic steam reforming was 0.42 g g_{plastic}⁻¹, while those from biochar steam gasification and RDF char–steam gasification were 0.30 and 0.10 g g_{plastic}⁻¹, respectively. Therefore, when biochar and RDF char were used as catalysts, the maximum theoretical hydrogen yields in the process were 0.72 and 0.52 g g_{plastic}⁻¹, respectively.

The ratio of experimental hydrogen yield to maximum theoretical hydrogen yield can represent the hydrogen potential of the process under different experimental conditions. Figure 5 shows the hydrogen potential in relation to the different catalyst temperatures and in relation to biochar and RDF char catalysts.

As can be seen from Figure 5, at low temperatures, the hydrogen potential for the pyrolysis-catalytic processing of HDPE using biochar as the catalyst was higher than that of RDF char. However, when the catalyst temperature was increased to 1000 °C, using RDF char as the catalyst resulted in the production of 60% of the hydrogen potential, which was higher than that produced using biochar as the catalyst, indicating that RDF char showed better catalytic hydrogen production ability at 1000 °C. Compared with biochar, RDF char contained more inorganic species (Table 1), which mainly existed in the form of K₃Na(SO₄)₂, Na(AlSi₃O₈), and CaCO₃. SEM-EDXS analysis showed that these inorganic species were evenly and well distributed on the surface of the char (Figure 2), which enabled the pyrolysis volatiles to be in full contact with the inorganic components of char, thus greatly increasing the hydrogen potential. This is consistent with the work of Mei et al.²⁸ who reported that MSW char was more active than wheat straw char in reforming biomass pyrolysis volatiles.

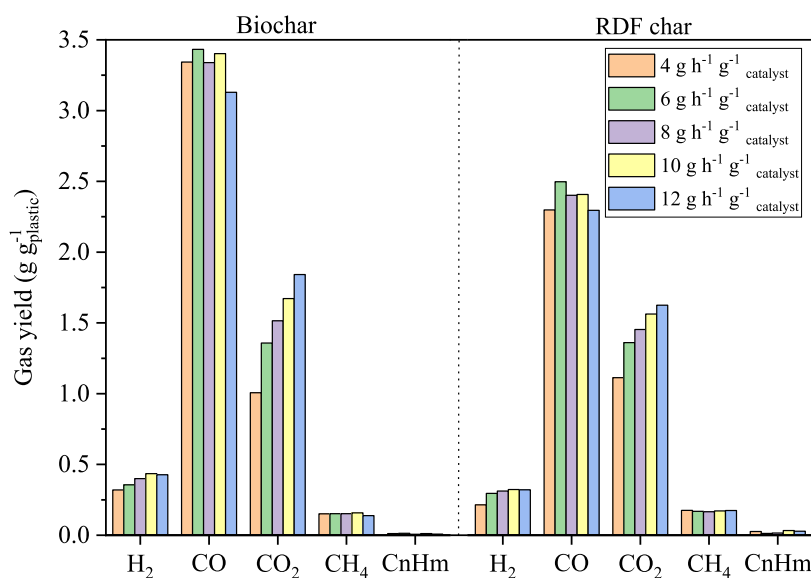
3.3. Influence of Steam Input on H₂ and Syngas Yield.

It has been reported that thermal cracking of pyrolysis oils is difficult.⁴⁰ However, the introduction of steam with high temperature can completely convert volatile hydrocarbons into CO and H₂.³⁷ To investigate the catalytic performance of biochar and RDF char at different steam inputs and the influence on the gas yield and gas composition, different steam weight hourly space velocities ranging from 4 to 12 g h⁻¹ g_{catalyst}⁻¹ were investigated. The HDPE plastic was pyrolyzed as before at a maximum pyrolysis temperature of 600 °C and the char catalysts were maintained at a catalytic steam reforming temperature of 1000 °C in the presence of either biochar or RDF char.

The gas yield, amount of reacted water, and amount of reacted char in relation to the different steam inputs are shown in Table 3. The results show that when biochar and RDF char

Table 3. Product Yields, Water Reacted, and Char Reacted in the Experiments at Different Steam Inputs with the Presence of Biochar and RDF Char

| steam weight hourly space velocity ($\text{g h}^{-1} \text{g}_{\text{catalyst}}^{-1}$) | 4 | | 6 | | 8 | | 10 | | 12 | |
|--|---------|----------|---------|----------|---------|----------|---------|----------|---------|----------|
| catalyst | biochar | RDF char |
| gas yield in relation to plastic + water + reacted char (wt %) | 81.9 | 73.9 | 67.5 | 58.3 | 56.5 | 46.6 | 48.6 | 40.9 | 40.9 | 33.8 |
| liquid yield in relation to plastic + water + reacted char (wt %) | 18.8 | 33.6 | 29.1 | 44.1 | 38.9 | 48.9 | 49.4 | 57.7 | 55.7 | 63.6 |
| mass balance (wt %) | 101.8 | 108.4 | 97.0 | 103.0 | 95.7 | 96.0 | 98.5 | 99.1 | 97.0 | 97.8 |
| gas yield ($\text{g g}_{\text{plastic}}^{-1}$) | 4.83 | 3.83 | 5.31 | 4.34 | 5.41 | 4.35 | 5.68 | 4.50 | 5.54 | 4.44 |
| syngas yield ($\text{g g}_{\text{plastic}}^{-1}$) | 3.66 | 2.51 | 3.78 | 2.79 | 3.73 | 2.71 | 3.83 | 2.73 | 3.55 | 2.61 |
| water reacted (g) | 2.74 | 1.9 | 3.58 | 2.59 | 3.86 | 3.15 | 3.91 | 3.31 | 4 | 3.14 |
| char reacted (g) | 1 | 0.54 | 1 | 0.61 | 1 | 0.62 | 1 | 0.62 | 1 | 0.65 |

**Figure 6.** Individual gas yield from pyrolysis-catalytic steam reforming of HDPE at different steam inputs in the presence of biochar and RDF char catalysts.

are used as catalysts, the gas yield in relation to plastic only and syngas yield increased first and then decreased with increasing steam input. For example, the total gas yield in relation to the amount of plastic input only from HDPE plastic using biochar as the catalyst increased from $4.83 \text{ g g}_{\text{plastic}}^{-1}$ at $4 \text{ g h}^{-1} \text{g}_{\text{catalyst}}^{-1}$ steam input to a maximum of $5.68 \text{ g g}_{\text{plastic}}^{-1}$ at $10 \text{ g h}^{-1} \text{g}_{\text{catalyst}}^{-1}$ steam input, but then decreased as the steam input was increased further. The RDF char also showed a similar total gas yield trend but at a lower total gas yield compared to biochar, where the maximum yield occurred at $10 \text{ g h}^{-1} \text{g}_{\text{catalyst}}^{-1}$ steam input with $4.50 \text{ g g}_{\text{plastic}}^{-1}$ of gas produced. The yield of syngas (H_2 and CO) also followed this same trend where the maximum yield of syngas at the steam input of $10 \text{ g h}^{-1} \text{g}_{\text{catalyst}}^{-1}$ was produced at $3.83 \text{ g g}_{\text{plastic}}^{-1}$ for biochar and $2.73 \text{ g g}_{\text{plastic}}^{-1}$ for RDF char. The decrease in yields at higher steam inputs has been noted before and attributed to surface saturation of the catalyst, restricting access of the pyrolysis volatiles to the active sites of the catalyst.^{41,42}

Under the same experimental conditions, the amount of water consumed in the experiment with biochar as the catalyst was higher than that of RDF char as the catalyst. It is worth noting that with different steam inputs, biochar was completely consumed and was converted to gas, whereas the RDF char consumption tended to be stable with the amount of reacted char being between 0.54 and 0.65 g, resulting in the production

of a high mass of ash residue (0.46–0.35 g of ash from 1 g of RDF char). Thereby, char consumption was similar with different steam inputs, suggesting that the gas yield was mainly due to more steam participating in the steam reforming reaction of hydrocarbons.

Figure 6 shows the individual gas yields from the pyrolysis-catalytic steam reforming of HDPE at different steam inputs with biochar and RDF char catalysts. When biochar was used as the catalyst, the H_2 yield increased linearly with the increase of steam input and reached a maximum of $0.43 \text{ g g}_{\text{plastic}}^{-1}$ at a steam input of $10 \text{ g h}^{-1} \text{g}_{\text{catalyst}}^{-1}$. Similarly, CO_2 yield increased with the increase of steam input because when steam was abundant, the water–gas shift reaction and char–steam reaction were enhanced to produce more H_2 and CO_2 . In this process, the yield of CO did not change significantly. The CH_4 and C_nH_m yields remained stable at 0.15 and $0.01 \text{ g g}_{\text{plastic}}^{-1}$, respectively, and did not change significantly under different steam input conditions. It can be seen that the steam reforming of CH_4 and C_nH_m was not affected when the steam input exceeded $4 \text{ g h}^{-1} \text{g}_{\text{catalyst}}^{-1}$. The pyrolysis volatiles generated in the first stage, particularly those of high molecular weight, may form carbonaceous deposits that could block the active reactive sites on the char surface and within the pore structures inside the catalyst. However, in the presence of steam and with high temperatures, these carbonaceous

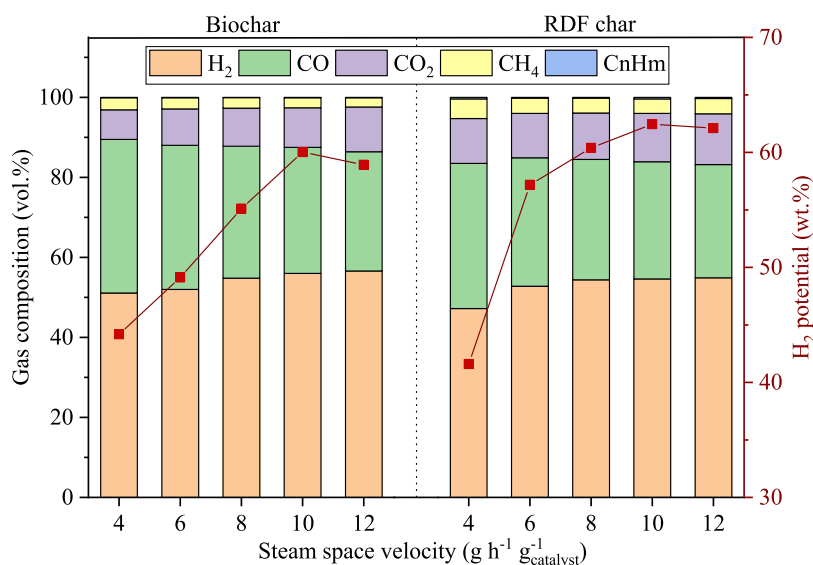


Figure 7. Volumetric gas composition and theoretical hydrogen yield production from pyrolysis-catalytic steam reforming of HDPE at different steam inputs in the presence of biochar and RDF char catalysts.

Table 4. Products Yield and Char Reacted from Pyrolysis-Catalytic Steam Reforming of Different Plastics in the Presence of Biochar and RDF Char Catalysts

| plastics | HDPE | | LDPE | | PP | | PS | | PET | |
|---|---------|----------|---------|----------|---------|----------|---------|----------|---------|----------|
| | biochar | RDF char |
| gas yield in relation to plastic + water + char (wt %) | 48.6 | 40.9 | 45.0 | 40.3 | 49.3 | 39.2 | 43.6 | 33.0 | 35.3 | 24.5 |
| liquid yield in relation to plastic + water + reacted char (wt %) | 49.4 | 57.7 | 50.3 | 58.2 | 49.4 | 61.2 | 49.1 | 59.3 | 56.3 | 62.9 |
| mass balance (wt %) | 98.5 | 99.1 | 95.9 | 98.9 | 98.7 | 100.9 | 92.8 | 92.7 | 93.0 | 89.1 |
| gas yield ($\text{g g}_{\text{plastic}}^{-1}$) | 5.68 | 4.50 | 5.29 | 4.5 | 5.7 | 4.4 | 5.03 | 3.74 | 4.15 | 2.84 |
| syngas yield ($\text{g g}_{\text{plastic}}^{-1}$) | 3.83 | 2.73 | 3.49 | 2.82 | 3.66 | 2.74 | 3.01 | 1.94 | 2.26 | 1.28 |
| char reacted (g) | 1 | 0.62 | 1 | 0.62 | 1 | 0.62 | 1 | 0.61 | 1 | 0.62 |

deposits can be transformed into gas, and the increase of steam input accelerated this transformation of the carbonaceous deposits. The increase in H_2 production was due to conversion of the carbonaceous deposits and also steam gasification of the char in addition to the hydrocarbon volatile steam reforming reactions.

When RDF char was used as the catalyst, the trend in the variation of gas yield of the individual gases in relation to steam input was similar to that when biochar was used as the catalyst, but the H_2 yield was significantly lower. For example, the maximum hydrogen yield from processing HDPE with RDF char was $0.32 \text{ g g}_{\text{plastic}}^{-1}$ with a steam input of $10 \text{ g h}^{-1} \text{ g}_{\text{catalyst}}^{-1}$ compared with $0.43 \text{ g g}_{\text{plastic}}^{-1}$ for biochar at the same steam input. The difference in gas yields between the two char catalysts derived from waste pyrolysis was attributed to differences in their catalytic activity on steam reforming of hydrocarbons and tar. The other factor was that the elemental composition and fixed carbon content (Table 1) of the two types of char were not the same, leading to different mass of carbon involved in the reaction, consequently influencing the overall gas yield.

Figure 7 shows the volumetric gas composition and H_2 potential for the pyrolysis-catalytic steam reforming of HDPE at different steam inputs in the presence of biochar and RDF char catalysts. As can be seen from Figure 7, the H_2 concentration in the gas mixture increased with the increase in steam input. When biochar was used as the catalyst, the

relative volumetric H_2 concentration was higher than that of RDF char catalyst under the same experimental conditions and reached 56 vol % at $12 \text{ g h}^{-1} \text{ g}_{\text{catalyst}}^{-1}$. Syngas concentration decreased slightly from 89.5 to 86.4 vol % when biochar was used as the catalyst, while syngas concentration remained between 83.5 and 84.5 vol % when RDF char was used as the catalyst. The increase in CO_2 concentration was mainly due to the reaction of carbon with steam to produce CO_2 (eq 5) rather than CO (eq 4) when steam was abundant.

In terms of the hydrogen potential, when using biochar as the catalyst, the experimental H_2 yield can reach 60% of the maximum theoretical H_2 yield at $10 \text{ g h}^{-1} \text{ g}_{\text{catalyst}}^{-1}$ steam input. When RDF char was used as the catalyst, the ratio of experimental H_2 yield to the maximum theoretical H_2 yield increased rapidly at first and then slowed. With increased steam input, the hydrogen potential yield can reach 62% of the maximum theoretical H_2 yield. When steam input was high, the RDF char showed a higher catalytic hydrogen production capacity than biochar in pyrolysis-catalytic steam reforming of HDPE.

3.4. Influence of Different Types of Plastics on H_2 and Syngas Yield. The type and compositional range of pyrolysis volatiles released during the first-stage pyrolysis of the waste plastic will depend on the structure and chemical composition of the plastic feedstock.²⁷ The consequent evolved volatiles will enter the second-stage pyrolysis-catalytic steam reforming process and will produce a different product distribution

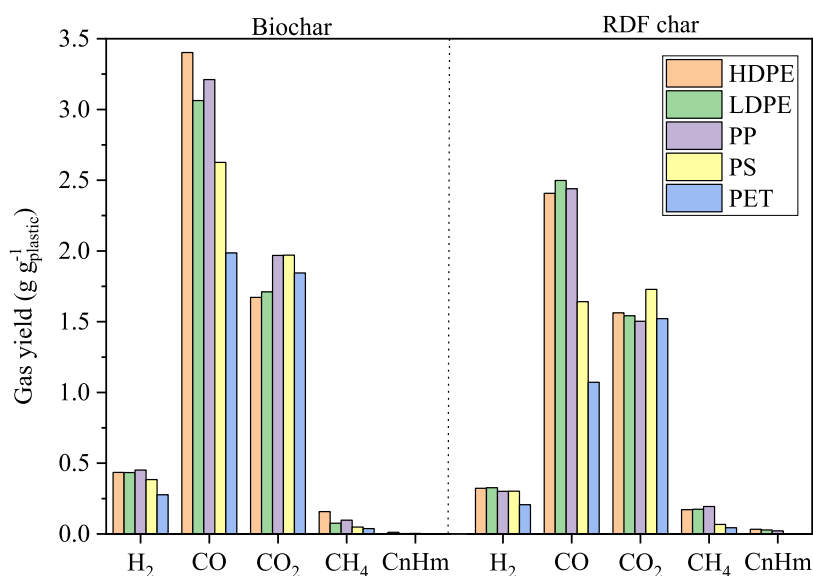


Figure 8. Individual gas yield from pyrolysis-catalytic steam reforming of different plastics in the presence of biochar and RDF char catalysts.

depending on the type of plastic feedstock. To study the effects of the biochar and RDF char catalysts on the pyrolysis-catalytic steam reforming behavior and the product distribution of different plastics, five different plastics, HDPE, LDPE, PP, PS, and PET were used as feedstock. The plastics chosen for investigation are among the most common plastics found in the plastics waste stream.¹ The process conditions used to investigate the different types of waste plastic were fixed at a catalytic temperature of 1000 °C and a weight hourly space velocity of 10 g h⁻¹ g_{catalyst}⁻¹ in the presence of biochar and RDF char catalysts. Table 4 shows the total gas yield and syngas (H₂ and CO) yield from the pyrolysis-catalytic steam reforming of different plastics in the presence of char catalysts presented on the basis of the mass of input plastic + water input + char and also in terms of the mass of plastic only. Also shown is the consumption of char catalysts during the catalytic process.

As can be seen from Table 4, when biochar was used as the catalyst, the total gas yield from pyrolysis-catalytic steam reforming of different plastics was higher than that produced using the RDF char as the catalyst under the same conditions. In addition, the polyalkene plastics, HDPE, LDPE, and PP produced high total gas yield and syngas yields with both the biochar and RDF char catalysts. However, PS with a very different chemical structure compared to polyalkenes and PET with different chemical compositions and different chemical structures produced significantly lower total gas and syngas yields. When biochar was used as the catalyst, the gas yield from processing PP was the highest, reaching 49.3 wt %, followed by HDPE, but PET had the lowest gas yield, at 35.3 wt %. When the RDF char was used as the catalyst, HDPE had the highest gas yield of 40.9 wt %, and LDPE and PP had slightly lower gas yields, while PET produced the lowest gas yield of 24.5 wt %.

The polyalkene plastics, HDPE, LDPE, and PP thermally degrade along the linear polymer structure, resulting in the formation of polymer fragments of a wide range of molecular weights. Therefore, the volatile oils and gases produced from pyrolysis of the polyalkene plastics are aliphatic in composition, consisting of alkanes, alkenes, and alkadienes.⁴³ Because of the presence of the aromatic ring in polystyrene,

pyrolysis produces a volatile product slate consisting of mainly styrene, and also toluene, xylene, and alkylated benzenes, indene, and indane. The thermal degradation of PET is influenced by the presence of oxygen and an aromatic ring in the polymer structure, and during pyrolysis generates large yield of carbon oxides, organic acids, and oxygenated hydrocarbons such as benzoic acid.⁴⁴

HDPE, LDPE, and PP had similar chemical structures and elemental composition, which made the composition of the evolved pyrolysis volatiles also similar. Therefore, the gas yield and composition in the catalytic steam reforming stage was similar. However, the chemical structures of PS and PET generated some volatile compounds such as styrene and benzoic acid with low conversion rates in the catalytic steam reforming process.⁷ As for the reactions of the char catalyst, it can be seen that at 1000 °C, the biochar was completely consumed and converted into gas in the catalytic process, but for the RDF char catalyst, there was 40 wt % of residual ash produced, derived from the high ash content of the char catalyst. Therefore, all of the carbon content of the RDF char catalyst was consumed by steam-char gasification.

The individual gas yields produced from the pyrolysis-catalytic steam reforming of the different plastic types using biochar and RDF char as the catalyst are shown in Figure 8. When using biochar as the catalyst, the H₂ yield from processing PP was the highest at 0.45 g g_{plastic}⁻¹, followed by HDPE and LDPE at around 0.43 g g_{plastic}⁻¹, while PET had the lowest H₂ yield at 0.27 g g_{plastic}⁻¹. Wu and Williams,⁴⁵ investigated the pyrolysis-gasification of different plastics with Ni-Mg-Al catalysts and reported that HDPE and PP had a similar H₂ yield at around 0.26 g g_{plastic}⁻¹, while the H₂ yield from PS was only 0.18 g g_{plastic}⁻¹. Hydrogen was produced mainly from steam reforming of the plastic pyrolysis volatiles and steam gasification of char catalysts. When the same catalyst was used, the H₂ yield was mainly determined by the structure and elemental composition of plastics. According to eqs 1 and 2, it can be seen that the content of elemental carbon and hydrogen in the pyrolysis volatiles increased the H₂ yield, while the presence of oxygen elements reduced the H₂ generation. PET had the lowest C and H content of the five plastics studied and contained 35 wt % oxygen. In addition, functional

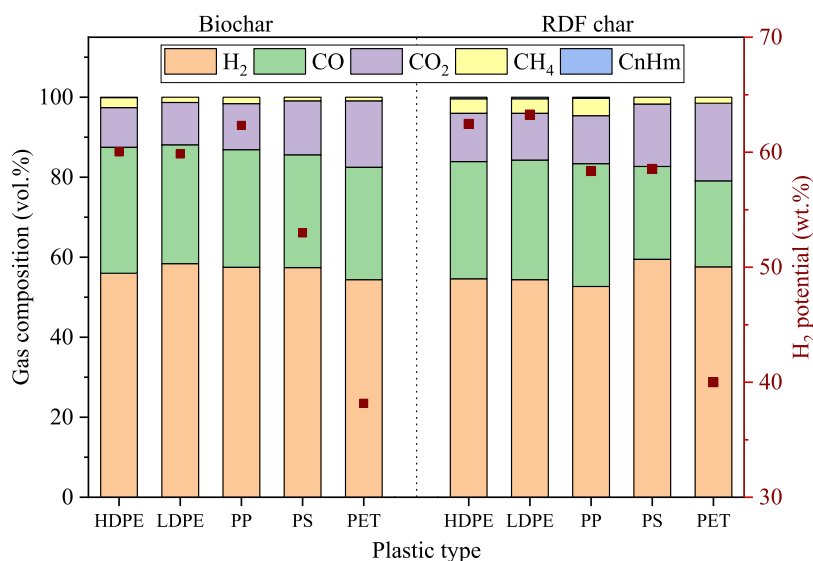


Figure 9. Volumetric gas composition and theoretical hydrogen yield production from pyrolysis-catalytic steam reforming of different plastics in the presence of biochar and RDF char catalysts.

groups on the polymeric skeleton of PET resulted in a yield of about 17 wt % of carbonaceous deposits during the pyrolysis stage. As a result, the H₂ yield from processing PET was the lowest. Carbon monoxide was also produced from the steam reforming of pyrolysis volatiles and steam gasification of the char catalysts. The CO yield of PS and PET was lower than that of the other three polyalkene plastics.

By comparing individual gas yields in the presence of biochar and RDF char, it can be seen that the yields of H₂, CO, and CO₂ were lower when the RDF char was used as the catalyst compared with the biochar catalyst under the same condition. However, Mei et al.²⁸ compared the role of MSW char and biochar for the steam reforming process of volatiles derived from the pyrolysis of MSW and wheat straw, and the results showed that MSW char was more active than biochar in reforming the volatile matter at 500–700 °C, resulting in higher gas yield. The research of Mei et al.²⁸ was carried out at a low temperature of 500–700 °C, and only a small amount of char catalyst was consumed. However, in the research reported here for the different plastics investigation, the catalyst temperature was 1000 °C, where all of the carbon in the char catalyst was converted into gas, thereby, significantly contributing to the gas yield. The high ash content in the RDF char resulted in a lower gas yield from RDF char–steam gasification compared with biochar steam gasification. However, when the RDF char was used as the catalyst, the yield of CH₄ was higher than that when biochar was used, mainly because the inorganic elements in RDF promoted the methanation of syngas. In a later study on syngas methanation, Mei et al.⁴⁶ pointed out that the inherent inorganic components in MSW char acted as a promoter for methanation because its composition is similar to the exogenous promoter used to modify the catalyst for methanation.

Figure 9 shows the volumetric gas composition from the pyrolysis-catalytic steam reforming of the different plastic types in the presence of biochar and RDF char. As can be seen from Figure 9, H₂ concentrations from LDPE, PP, and PS were similar at around 58 vol % when biochar was used as the catalyst. Although the gas yield and hydrogen yield of PS and

PET were much lower than those of the other three plastics, the relative volumetric H₂ concentration was not much different. According to eqs 1 and 2, it can be seen that the presence of oxygen in the feedstock resulted in the product of steam reforming as CO₂, while that of C_nH_m was CO, which also explained the high content of CO₂ in the gas composition from PET.

When RDF char was used as the steam reforming catalyst, the volumetric H₂ concentrations from HDPE, LDPE, and PP were slightly lower than those using biochar as the catalyst, while the H₂ concentrations from PS and PET were higher (Figure 9). This may be due to the fact that the high inorganic content of RDF char was more evident for the steam reforming of aromatic and oxygenated hydrocarbons. Methane concentrations were also higher than when biochar was used as a catalyst due to the methanation of H₂ and CO in the syngas.

The hydrogen potential, comparing the experimental H₂ yield from the pyrolysis-catalytic steam reforming of the different plastics in relation to the calculated maximum theoretical H₂ yield is also shown in Figure 9. It can be seen that when biochar was used as the catalyst, the H₂ potential of PP was the highest at ~62%, followed by HDPE and LDPE at ~60%, then followed by PS at ~53%, while the hydrogen yield of PET only reached 38% of the maximum hydrogen yield. When RDF char was used as the catalyst, the hydrogen potential was higher than that when biochar was used as the catalyst, especially for the steam reforming of PS and PET. This suggests that the minerals, especially those with a high content of nonorganically bound metals in minerals in the RDF char can promote the conversion of oxygenated compounds into more easily reformed hydrocarbons. Mei et al.²⁸ also pointed out that the oil products from catalytic steam reforming of biomass pyrolysis volatiles using biochar as the catalyst contained higher oxygenated compounds. However, MSW char can convert oxygenated compounds into aliphatic hydrocarbons and inhibit the generation of polycyclic aromatic hydrocarbons. CaO has also been shown to have a strong catalytic effect on the cracking of aromatic rings in pyrolysis volatiles.³¹

This work has shown that carbonaceous chars produced from the slow pyrolysis of waste materials in the form of biomass waste and processed municipal solid waste can act as effective catalysts for the production of a hydrogen-rich syngas from waste plastics. Enormous tonnages of wastes suitable to act as feedstock for the production of pyrolysis bio-oils are generated worldwide each year, which include agricultural and forestry biomass waste, municipal solid waste, and urban wood waste. The potential production of bio-oils from such wastes is established as a route to produce future fuels from a renewable source. However, biochar, a byproduct of pyrolysis bio-oil production, requires an end-use application, which may be limited, particularly if waste-derived biomass sources are used because they may contain high levels of alkali, alkaline-earth, and/or transition metals. However, the use of waste-derived chars as a catalyst for the steam reforming of waste plastics volatiles represents a novel application resulting in the production of a higher-value product, namely, hydrogen. A further advantage of the use of a relatively low-cost waste-derived char as a catalyst is that it is consumed during the process via char–steam gasification reactions, further increasing the production of hydrogen and syngas. The char therefore acts as both a catalyst and a reactant.

The commercial production of hydrogen is almost exclusively from fossil fuel natural gas (76%) and coal (23%).⁴⁷ For natural gas, which is composed of methane (≥ 95 mol %) and other C_1 – C_5 hydrocarbons, the most common large-scale process used for hydrogen production is natural gas catalytic steam reforming. The process has some similarities with the process described in this work in that a range of hydrocarbons are produced in the first-stage pyrolysis of the plastics, followed by catalytic steam reforming in the second stage using a char-based catalyst. However, the range of hydrocarbons produced from waste plastics would be very much more complex, particularly if mixed plastics were used that would generate a range of volatile hydrocarbons containing aromatic and aliphatic species and also potentially oxygenated species, nitrogen-, sulfur-, chlorine-containing hydrocarbons, etc. Such species can poison and deactivate the steam reforming catalyst. In addition, the commercial catalytic steam reforming process takes place under process conditions of temperature between 700 and 1000 °C and at pressures of 0.3–2.5 MPa. The products from the reformer are composed of H_2 and CO and are passed to two water–gas shift reactors in series where the CO is converted to CO_2 and H_2 (eq 3). The high-temperature shift reactor typically operates with a Fe-based catalyst at temperatures of 310–450 °C and the low-temperature shift reactor operates with a Cu-based catalyst and at temperatures of 200–250 °C. Clearly, the process conditions for reforming and water–gas shift reactions that are optimized for the commercial process are not the same as those used in the second-stage reactor in this work. Importantly, the catalytic steam reforming reactions, water–gas shift reactions, and steam–carbon gasification reactions all occur in one place in the second-stage reactor. Therefore, the reactions would be much more complex than the equilibrium reactions described by eqs 1–6. Further development of the process should include work on a wide range of different “real-world” plastics to determine the influence of contamination and the influence of catalyst poisoning and deactivation. Also, the introduction of separate third water–gas shift reactors, which could be optimized for the conversion of carbon

monoxide to hydrogen via the water–gas shift process, has been recently investigated.⁴⁸

4. CONCLUSIONS

In this paper, two different char catalysts (biochar and RDF char) were compared to understand their catalytic performance in relation to the steam reforming of pyrolysis volatiles produced from waste plastics at different process parameters. The role of temperature in the catalytic steam reforming of pyrolysis volatiles was investigated. The H_2 yield from the processing of HDPE with the biochar catalyst increased linearly from 0.13 to 0.36 $g_{plastic}^{-1}$ as the catalyst temperature was increased from 800 to 1000 °C. This was due to the simultaneous reactions of hydrocarbon reforming and char “sacrificial” gasification. At high temperatures, the introduction of steam completely converted the hydrocarbon volatiles to H_2 and CO. When biochar and RDF char were used as catalysts, the maximum H_2 yields were 0.43 and 0.32 $g_{plastic}^{-1}$, respectively, at a steam input of 10 $g_{catalyst}^{-1} h^{-1}$.

The hydrogen potential was used to compare the catalytic properties of the two different catalysts for HDPE processing under the same experimental conditions. The results showed that at 1000 °C, the hydrogen potential of the RDF char catalyst was generally higher than that of biochar as the catalyst, mainly because RDF char contains more inorganic species with catalytic properties. In addition, RDF char showed a strong catalytic effect for reforming oxygen compounds and aromatic rings in the volatiles of PET and PS pyrolysis.

Polyalkene plastics (HDPE, LDPE, and PP) showed a hydrogen potential of between 60 and 62%, whereas the aromatic structured polystyrene was 53% and the oxygenated, aromatic structured PET produced a hydrogen potential of 38%.

AUTHOR INFORMATION

Corresponding Author

Paul T. Williams – School of Chemical and Process Engineering, University of Leeds, Leeds LS2 9JT, U.K.;
orcid.org/0000-0003-0401-9326; Phone: #44 1133432504; Email: p.t.williams@leeds.ac.uk

Author

Yukun Li – School of Chemical and Process Engineering, University of Leeds, Leeds LS2 9JT, U.K.

Complete contact information is available at:
<https://pubs.acs.org/10.1021/acs.iecr.3c02292>

Notes

The authors declare no competing financial interest.

ACKNOWLEDGMENTS

Y.L. was awarded a China Scholarship Council-University of Leeds scholarship to carry out the research that is gratefully acknowledged.

REFERENCES

- (1) PlasticsEurope 2022. *Plastics the Facts 2022*; PlasticsEurope: Brussels, Belgium, 2022.
- (2) Geyer, R.; Jambeck, J. R.; Law, K. L. Production, use, and fate of all plastics ever made. *Sci. Adv.* **2017**, *3*, No. e1700782.
- (3) Jahirul, M.; Rasul, M.; Schaller, D.; Khan, M.; Hasan, M.; Hazrat, M. Transport fuel from waste plastics pyrolysis—A review on

technologies, challenges and opportunities. *Energy Convers. Manage.* **2022**, *258*, No. 115451.

(4) Williams, P. T. Hydrogen and carbon nanotubes from pyrolysis-catalysis of waste plastics: A review. *Waste Biomass Valorization* **2021**, *12*, 1–28.

(5) Lopez, G.; Artetxe, M.; Amutio, M.; Bilbao, J.; Olazar, M. Thermochemical routes for the valorization of waste polyolefinic plastics to produce fuels and chemicals. A review. *Renewable Sustainable Energy Rev.* **2017**, *73*, 346–368.

(6) Lopez, G.; Artetxe, M.; Amutio, M.; Alvarez, J.; Bilbao, J.; Olazar, M. Recent advances in the gasification of waste plastics. A critical overview. *Renewable Sustainable Energy Rev.* **2018**, *82*, 576–596.

(7) Barbarias, I.; Lopez, G.; Artetxe, M.; Arregi, A.; Bilbao, J.; Olazar, M. Valorisation of different waste plastics by pyrolysis and in-line catalytic steam reforming for hydrogen production. *Energy Convers. Manage.* **2018**, *156*, 575–584.

(8) Jiang, Y.; Li, X.; Li, C.; Zhang, L.; Zhang, S.; Li, B.; Wang, S.; Hu, X. Pyrolysis of typical plastics and coupled with steam reforming of their derived volatiles for simultaneous production of hydrogen-rich gases and heavy organics. *Renewable Energy* **2022**, *200*, 476–491.

(9) Cortazar, M.; Gao, N.; Quan, C.; Suarez, M. A.; Lopez, G.; Orozco, S.; Santamaria, L.; Amutio, M.; Olazar, M. Analysis of hydrogen production potential from waste plastics by pyrolysis and in line oxidative steam reforming. *Fuel Process. Technol.* **2022**, *225*, No. 107044.

(10) Zhang, Y.; Huang, J.; Williams, P. T. Fe–Ni–MCM-41 catalysts for hydrogen-rich syngas production from waste plastics by pyrolysis–catalytic steam reforming. *Energy Fuels* **2017**, *31*, 8497–8504.

(11) Yao, D.; Yang, H.; Chen, H.; Williams, P. T. Investigation of nickel-impregnated zeolite catalysts for hydrogen/syngas production from the catalytic reforming of waste polyethylene. *Appl. Catal., B* **2018**, *227*, 477–487.

(12) Wu, C.; Williams, P. T. Investigation of Ni–Al, Ni–Mg–Al and Ni–Cu–Al catalyst for hydrogen production from pyrolysis–gasification of polypropylene. *Appl. Catal., B* **2009**, *90*, 147–156.

(13) Yao, D.; Hu, Q.; Wang, D.; Yang, H.; Wu, C.; Wang, X.; Chen, H. Hydrogen production from biomass gasification using biochar as a catalyst/support. *Bioresour. Technol.* **2016**, *216*, 159–164.

(14) Santamaria, L.; Lopez, G.; Fernandez, E.; Cortazar, M.; Arregi, A.; Olazar, M.; Bilbao, J. Progress on catalyst development for the steam reforming of biomass and waste plastics pyrolysis volatiles: a review. *Energy Fuels* **2021**, *35*, 17051–17084.

(15) Ashok, J.; Dewangan, N.; Das, S.; Hongmanorom, P.; Wai, M. H.; Tomishige, K.; Kawi, S. Recent progress in the development of catalysts for steam reforming of biomass tar model reaction. *Fuel Process. Technol.* **2020**, *199*, No. 106252.

(16) Gao, N.; Wang, F.; Quan, C.; Santamaria, L.; Lopez, G.; Williams, P. T. Tire pyrolysis char: Processes, properties, upgrading and applications. *Prog. Energy Combust. Sci.* **2022**, *93*, No. 101022.

(17) Xiong, X.; Iris, K.; Cao, L.; Tsang, D. C.; Zhang, S.; Ok, Y. S. A review of biochar-based catalysts for chemical synthesis, biofuel production, and pollution control. *Bioresour. Technol.* **2017**, *246*, 254–270.

(18) Li, Y.; Nahil, M. A.; Williams, P. T. Pyrolysis-catalytic steam reforming of waste plastics for enhanced hydrogen/syngas yield using sacrificial tire pyrolysis char catalyst. *Chem. Eng. J.* **2023**, *467*, No. 143427.

(19) Li, Y.; Nahil, M. A.; Williams, P. T. Hydrogen/syngas production from different types of waste plastics using a sacrificial tire char catalyst via pyrolysis–catalytic steam reforming. *Energy Fuels* **2023**, *37*, 6661–6673.

(20) Liu, Y.; Paskevicius, M.; Wang, H.; Parkinson, G.; Veder, J.-P.; Hu, X.; Li, C.-Z. Role of O-containing functional groups in biochar during the catalytic steam reforming of tar using the biochar as a catalyst. *Fuel* **2019**, *253*, 441–448.

(21) Klinghoffer, N. B.; Castaldi, M. J.; Nzihou, A. Influence of char composition and inorganics on catalytic activity of char from biomass gasification. *Fuel* **2015**, *157*, 37–47.

(22) Wang, Y.; Huang, L.; Zhang, T.; Wang, Q. Hydrogen-rich syngas production from biomass pyrolysis and catalytic reforming using biochar-based catalysts. *Fuel* **2022**, *313*, No. 123006.

(23) Wang, B.-S.; Cao, J.-P.; Zhao, X.-Y.; Bian, Y.; Song, C.; Zhao, Y.-P.; Fan, X.; Wei, X.-Y.; Takarada, T. Preparation of nickel-loaded on lignite char for catalytic gasification of biomass. *Fuel Process. Technol.* **2015**, *136*, 17–24.

(24) Al-Rahbi, A. S.; Williams, P. T. Hydrogen-rich syngas production and tar removal from biomass gasification using sacrificial tyre pyrolysis char. *Appl. Energy* **2017**, *190*, 501–509.

(25) Gerassimidou, S.; Velis, C. A.; Williams, P. T.; Komilis, D. Characterisation and composition identification of waste-derived fuels obtained from municipal solid waste using thermogravimetry: A review. *Waste Manage. Res.* **2020**, *38*, 942–965.

(26) Czernik, S.; French, R. J. Production of hydrogen from plastics by pyrolysis and catalytic steam reform. *Energy Fuels* **2006**, *20*, 754–758.

(27) Soni, V. K.; Singh, G.; Vijayan, B. K.; Chopra, A.; Kapur, G. S.; Ramakumar, S. Thermochemical Recycling of Waste Plastics by Pyrolysis: A Review. *Energy Fuels* **2021**, *35*, 12763–12808.

(28) Mei, Z.; He, X.; Chen, D.; Wang, N.; Yin, L.; Qian, K.; Feng, Y. Comparison of chars from municipal solid waste and wheat straw for understanding the role of inorganics in char-based catalysts during volatile reforming process. *Energy* **2021**, *229*, No. 120619.

(29) Vassilev, S. V.; Baxter, D.; Andersen, L. K.; Vassileva, C. G. An overview of the composition and application of biomass ash. Part I. Phase–mineral and chemical composition and classification. *Fuel* **2013**, *105*, 40–76.

(30) Zhang, S.; Song, Y.; Song, Y. C.; Yi, Q.; Dong, L.; Li, T. T.; Zhang, L.; Feng, J.; Li, W. Y.; Li, C.-Z. An advanced biomass gasification technology with integrated catalytic hot gas cleaning. Part III: Effects of inorganic species in char on the reforming of tars from wood and agricultural wastes. *Fuel* **2016**, *183*, 177–184.

(31) Liu, X.; Xiong, B.; Huang, X.; Ding, H.; Zheng, Y.; Liu, Z.; Zheng, C. Effect of catalysts on char structural evolution during hydrogasification under high pressure. *Fuel* **2017**, *188*, 474–482.

(32) Sipra, A. T.; Gao, N.; Sarwar, H. Municipal solid waste (MSW) pyrolysis for bio-fuel production: A review of effects of MSW components and catalysts. *Fuel Process. Technol.* **2018**, *175*, 131–147.

(33) Al-Rahbi, A. S.; Onwudili, J. A.; Williams, P. T. Thermal decomposition and gasification of biomass pyrolysis gases using a hot bed of waste derived pyrolysis char. *Bioresour. Technol.* **2016**, *204*, 71–79.

(34) Franco, C.; Pinto, F.; Gulyurtlu, I.; Cabrita, I. The study of reactions influencing the biomass steam gasification process. *Fuel* **2003**, *82*, 835–842.

(35) Wu, W.-g.; Luo, Y.-h.; Chen, Y.; Su, Y.; Zhang, Y.; Zhao, S.; Wang, Y. Experimental investigation of tar conversion under inert and partial oxidation conditions in a continuous reactor. *Energy Fuels* **2011**, *25*, 2721–2729.

(36) Li, Q.; Wang, Q.; Kayamori, A.; Zhang, J. Experimental study and modeling of heavy tar steam reforming. *Fuel Process. Technol.* **2018**, *178*, 180–188.

(37) Jess, A. Mechanisms and kinetics of thermal reactions of aromatic hydrocarbons from pyrolysis of solid fuels. *Fuel* **1996**, *75*, 1441–1448.

(38) Yao, D.; Yang, H.; Chen, H.; Williams, P. T. Co-precipitation, impregnation and so-gel preparation of Ni catalysts for pyrolysis-catalytic steam reforming of waste plastics. *Appl. Catal., B* **2018**, *239*, 565–577.

(39) Chaudhari, S. T.; Bej, S.; Bakhshi, N.; Dalai, A. Steam gasification of biomass-derived char for the production of carbon monoxide-rich synthesis gas. *Energy Fuels* **2001**, *15*, 736–742.

(40) Bridgwater, A. The technical and economic feasibility of biomass gasification for power generation. *Fuel* **1995**, *74*, 631–653.

(41) Erkiaga, A.; Lopez, G.; Amutio, M.; Bilbao, J.; Olazar, M. Syngas from steam gasification of polyethylene in a conical spouted bed reactor. *Fuel* **2013**, *109*, 461–469.

(42) Simell, P. A.; Hirvensalo, E. K.; Smolander, V. T.; Krause, A. O. I. Steam reforming of gasification gas tar over dolomite with benzene as a model compound. *Ind. Eng. Chem. Res.* **1999**, *38*, 1250–1257.

(43) Williams, P. T. Yield and Composition of Gases and Oils/waxes from the Feedstock Recycling of Waste Plastic. In *Feedstock Recycling and Pyrolysis of Waste Plastics*; Schiers, J.; Kaminsky, W., Eds.; John Wiley & Sons Ltd.: Chichester, 2006; Chapter 11, pp 285–314.

(44) Artetxe, M.; Lopez, G.; Amutio, M.; Elordi, G.; Olazar, M.; Bilbao, J. Operating conditions for the pyrolysis of poly-(ethylene terephthalate) in a conical spouted-bed reactor. *Ind. Eng. Chem. Res.* **2010**, *49*, 2064–2069.

(45) Wu, C.; Williams, P. T. Pyrolysis–gasification of plastics, mixed plastics and real-world plastic waste with and without Ni–Mg–Al catalyst. *Fuel* **2010**, *89*, 3022–3032.

(46) Mei, Z.; Chen, D.; Qian, K.; Zhang, R.; Yu, W. Producing eco-methane with raw syngas containing miscellaneous gases and tar by using a municipal solid waste char-based catalyst. *Energy* **2022**, *254*, No. 124244.

(47) IEA. *The Future of Hydrogen; Seizing Today's Opportunities*; International Energy Agency: Paris, France, 2019.

(48) Alshareef, R.; Nahil, M. A.; Williams, P. T. Hydrogen production by three stage (i) pyrolysis (ii) catalytic steam reforming (iii) water gas shift processing of waste plastic. *Energy Fuels* **2023**, *37*, 3894–3907.